Results in Physics 6 (2016) 904–910

Contents lists available at ScienceDirect

Results in Physics

journal homepage: www.journals.elsevier.com/results-in-physics

Hydromagnetic mixed convection flow of copper and silver water nanofluids due to a curved stretching sheet

Tasawar Hayat [a,b], Asmara Kiran [a], Maria Imtiaz [a,*], Ahmed Alsaedi [b]

[a] Department of Mathematics, Quaid-I-Azam University 45320, Islamabad 44000, Pakistan

[b] Nonlinear Analysis and Applied Mathematics (NAAM) Research Group, Department of Mathematics, Faculty of Science, King Abdulaziz University, Jeddah 21589, Saudi Arabia

ARTICLE INFO

Article history:
Received 1 October 2016
Received in revised form 25 October 2016
Accepted 27 October 2016
Available online 9 November 2016

Keywords:
Magnetohydrodynamics (MHD)
Copper and silver water nanofluids
Mixed convection
Nonlinear thermal radiation
Joule heating

ABSTRACT

Main objective of present analysis is to study the MHD mixed convection flow of nanofluid due to a curved stretching sheet. Water based nanofluid comprising copper and silver as nanoparticles is used. Heat transfer analysis is carried out in the presence of Joule heating and nonlinear thermal radiation. Similarity transformations are used to obtain the system of nonlinear ordinary differential equations. Convergent series solutions are obtained. Effects of different variables on velocity and temperature are examined. Skin friction coefficient and Nusselt number are examined and analyzed for the influence of different involved parameters.

Introduction

Nanofluids are defined as addition of nanometer sized solid particles into the traditional heat transfer fluids that increase the thermal conductivity of the base fluid. Size of nanomaterials is between 1 and 100 nm. Firstly Choi [1] introduced the term nanofluid. Common base fluids used in nanofluids are water, ethylene glycol and oil. Nanofluids have many application in heat transfer including microelectronic, fuel cells, engine cooling vehicle, domestic and refrigerator. Nanofluid are significant in heat transfer rate to enhance the thermal properties such as electronic cooling system, radiators and heat exchanger. Nanofluids are used in automobiles as coolant because it increases the heat transfer rate. Nanoparticles have been made of different materials such as oxide ceramics, nitride oxide, metals, semiconductor and carbon nanotubes. Magnetic nanofluid is a fluid with unique characteristics of both liquid and magnetic field. Such fluids have been found to have several fascinating applications such as magneto-optical wavelength filter, optical modulators, nonlinear optical materials, tunable optical fiber filter, optical grating, optical switches etc. Magneto nanofluids are useful to guide the particles up the blood stream to a tumor with magnets because magnetic nanoparticles are more adhesive to tumor cells than non-malignant cells. Such particles absorb more power than microparticles in alternating current magnetic fields tolerable in humans i.e. for cancer therapy. Numerous applications involving magnetic nanofluids include drug delivery, contrast enhancement in magnetic resonance imaging and magnetic cell separation. Heat transfer augmentation in a two-sided lid-driven differentially heated square cavity utilizing nanofluids is examined by Tiwari and Das [2]. Turkyilmazoglu [3] discussed nanofluid flow due to a rotating disk. Vajravelu et al. [4] studied Ag-water and Cu-water nanofluids flow and convective heat transfer over a stretching sheet. MHD nanofluid flow subject to second order slip velocity and chemical reaction is investigated by Hayat et al. [5]. Sheikholeslami et al. [6] examined effect of thermal radiation on MHD nanofluid flow. Peristaltic transport of copper–water nanofluid saturating porous medium is illustrated by Abbasi et al. [7]. Hayat et al. [8] discussed effects of chemical reaction in flow of ferrofluid by a rotating disk. Mansur and Ishak [9] investigated unsteady nanofluid flow over a stretching sheet with a convective boundary condition.

Magnetohydrodynamics concern the dynamics of magnetic field in electrically conducting fluids. MHD are useful in many applications like engineering, medicine, geophysics and transportation. Physiological fluids, in sink float separation, blood pump machines and blood plasma are the fields in which MHD plays a great role. Effects of thermal radiation on MHD nanofluid flow over a convective stretching surface are discussed by Makinde et al. [10]. MHD nanofluid flow and heat transfer in a stretching channel considering thermal radiation are investigated by Dogonchi and Ganji [11]. Ibanez et al. [12] analyzed MHD nanofluid flow in

* Corresponding author.
E-mail address: mi_qau@yahoo.com (M. Imtiaz).

http://dx.doi.org/10.1016/j.rinp.2016.10.023
2211-3797/

porous microchannel with thermal radiation. Unsteady flow and heat transfer of nanofluid under the effect of magnetic field are discussed by Sheikholeslami et al. [13]. Influence of magnetic field in third grade fluid flow over a stretching surface has been examined by Asghar et al. [14].

Thermal radiation has wide application in polymer technology, food production, engineering and spinning of fibers and advanced energy conversion system in heat transfer at high temperature. Effect of thermal radiation is dominant when temperature difference becomes larger. Rashidi et al. [15] studied mixed convection heat transfer for viscoelastic fluid flow over a porous wedge with thermal radiation. Mukhopadhyay [16] presented slip effects on MHD boundary layer flow over an exponentially stretching sheet with suction/blowing and thermal radiation. Bhattacharyya et al. [17] examined radiative flow of micropolar fluid over a porous shrinking sheet. Second law analysis for variable viscosity hydromagnetic boundary layer flow with thermal radiation and Newtonian heating is investigated by Makinde [18]. Magyari [19] indicated that linear radiation problem for flow past a flat plate can be simply reduced to re-scaling of Prandtl number by a factor involving radiation parameter. It means that effect of linear radiation on flow and heat transfer characteristics is trivial both physically and computationally. Keeping this in view some researchers recently proposed the idea of nonlinear radiative heat transfer. It is seen that energy equation in the case of nonlinear radiation is strongly nonlinear and contains an additional temperature parameter which is the ratio of wall and ambient temperatures. Hayat et al. [20] discussed MHD flow of nanofluid in the presence of nonlinear thermal radiation. Impact of nonlinear thermal radiation on three dimensional flow of nanofluid has been analyzed by Hayat et al. [21]. Mustafa et al. [22] examined stagnation point flow of power law fluid with nonlinear thermal radiation. Effect of nonlinear thermal radiation in the flow of Jeffrey nanofluid is presented by Shehzad et al. [23]. Nanofluid flow in the presence of nonlinear thermal radiation has been illustrated by Mushtaq et al. [24]. Cortell [25] discussed the nonlinear thermal radiation over a stretching sheet. Sakiadis flow with nonlinear thermal radiation has been studied by Pantokratoras and Fang [26].

Present article investigates the effect of mixed convection and nonlinear thermal radiation on nanofluid flow past a curved stretching sheet. Effects of Joule heating are also taken into consideration. Homotopy analysis method [27–34] is used to obtain the convergent series solutions. Effects of different parameters on the velocity, temperature, skin friction coefficient and Nusselt number have been presented through graphs and analyzed.

Model development

Consider two-dimensional nanofluid flow by a curved unsteady stretching sheet coiled in a circle of radius R. Stretching of sheet is taken in the s-direction with the velocity $u = u_w = as$. A magnetic field of strength B_0 is applied in the r-direction. Also the bottom surface of sheet has temperature T_w while ambient fluid temperature is T_∞. Governing equations of present boundary layer flow problem are

$$\frac{\partial}{\partial r}\{(r+R)\mathrm{v}\} + R\frac{\partial u}{\partial s} = 0, \tag{1}$$

$$\frac{u^2}{r+R} = \frac{1}{\rho_{nf}}\frac{\partial p}{\partial r}, \tag{2}$$

$$\begin{aligned}\mathrm{v}\frac{\partial u}{\partial r} + \frac{Ru}{r+R}\frac{\partial u}{\partial s} + \frac{u\mathrm{v}}{r+R} = & -\frac{1}{\rho_{nf}}\frac{R}{r+R}\frac{\partial p}{\partial s} + \frac{\mu_{nf}}{\rho_{nf}}\left(\frac{\partial^2 u}{\partial r^2} + \frac{1}{r+R}\frac{\partial u}{\partial r} - \frac{u}{(r+R)^2}\right)\\ & - \frac{\sigma B_0^2}{\rho_{nf}(r+R)^2}u + \frac{g(\beta\rho)_{nf}}{\rho_{nf}}(T - T_\infty),\end{aligned} \tag{3}$$

$$\begin{aligned}\mathrm{v}\frac{\partial T}{\partial r} + \frac{uR}{r+R}\frac{\partial T}{\partial s} = & \alpha_{nf}\left(\frac{\partial^2 T}{\partial r^2} + \frac{1}{r+R}\frac{\partial T}{\partial r}\right) - \frac{1}{(\rho C_p)_{nf}(r+R)}\frac{\partial}{\partial r}\{(r+R)q_r\}\\ & + \frac{\sigma_{nf}B_0^2}{(\rho C_p)_{nf}}\left(\frac{u}{r+R}\right)^2,\end{aligned} \tag{4}$$

where $u(r,s)$ and $\mathrm{v}(r,s)$ are the velocity components, $\sigma$the electrical conductivity, p the pressure, B_0 the strength of magnetic field, g the gravitational acceleration and T the temperature.

Effective dynamic viscosity μ_{nf} of the nanofluid [35] is defined as:

$$\mu_{nf} = \frac{\mu_f}{(1-\varphi)^{2.5}}, \tag{5}$$

here φ denotes the solid volume fraction of nanoparticles. Nanofluid effective heat capacitance $(\rho C_p)_{nf}$, thermal diffusivity α_{nf}, density ρ_{nf} [2] and electrical conductivity σ_{nf} [36] are defined as:

$$(\rho C_p)_{nf} = (1-\varphi)(\rho C_p)_f + \varphi(\rho C_p), \tag{6}$$

$$\alpha_{nf} = \frac{k_{nf}}{(\rho C_p)_{nf}}, \tag{7}$$

$$\rho_{nf} = (1-\varphi)\rho_f + \varphi\rho_s, \tag{8}$$

$$\frac{\sigma_{nf}}{\sigma_f} = 1 + \frac{3\left(\frac{\sigma_s}{\sigma_f} - 1\right)\varphi}{\left(\frac{\sigma_s}{\sigma_f} + 2\right) - \left(\frac{\sigma_s}{\sigma_f} - 1\right)\varphi}. \tag{9}$$

For spherical shaped nanoparticles the Maxwell model defines thermal conductivity k_{nf} [37] as follows:

$$\frac{k_{nf}}{k_f} = \frac{k_s + 2k_f - 2\varphi(k_f - k_s)}{k_s + 2k_f + \varphi(k_f - k_s)}, \tag{10}$$

where nf, s and f in subscripts are for nanofluid, nano-solid particles and base fluid respectively.

Boundary conditions for the present problem are

$$\begin{aligned} & u = as, \quad \mathrm{v} = 0, \quad T = T_w \text{ at } r = 0,\\ & u \to 0, \quad \frac{\partial u}{\partial r} \to 0, \quad T \to T_\infty \text{ as } r \to \infty.\end{aligned} \tag{11}$$

Radiative heat flux by using the Rosseland approximation is defined as:

$$q_r = -\frac{4\sigma^*}{3k^*}\frac{\partial T^4}{\partial r} = -\frac{16\sigma^*}{3k^*}T^3\frac{\partial T}{\partial r}, \tag{12}$$

where σ^* the Stefan–Boltzmann constant and k^* the mean absorption coefficient. Using Eq. (11), Eq. (4) implies that

$$\begin{aligned}\mathrm{v}\frac{\partial T}{\partial r} + \frac{uR}{r+R}\frac{\partial T}{\partial s} = & \alpha_{nf}\left(\frac{\partial^2 T}{\partial r^2} + \frac{1}{r+R}\frac{\partial T}{\partial r}\right) - \frac{1}{(\rho C_p)_{nf}(r+R)}\\ & \times \frac{\partial}{\partial r}\left(-\frac{16\sigma^*}{3k^*}T^3\frac{\partial T}{\partial r}\right) + \frac{\sigma_{nf}B_0^2}{(\rho C_p)_{nf}}\left(\frac{u}{r+R}\right)^2,\end{aligned} \tag{13}$$

We introduce the following similarity transformations

$$\begin{aligned} & u = as\, f'(\eta), \ \mathrm{v} = \frac{-R}{r+R}\sqrt{a\nu_f}f(\eta), \ \eta = \sqrt{\frac{a}{\nu_f}}r,\\ & p = \rho a^2 s^2 P(\eta), \ \theta(\eta) = \frac{T - T_\infty}{T_w - T_\infty}.\end{aligned} \tag{14}$$

Using Eq. (14) continuity equation is satisfied automatically and Eqs. (2), (3) and (13) take the form:

$$\frac{\partial p}{\partial \eta} = \frac{f'^2}{\varphi_1(\eta + k)}, \tag{15}$$

$$\frac{2A\varphi_1}{(A+\eta)}P(\eta)=\beta_1\left(f'''+\frac{f''}{(A+\eta)}-\frac{f'}{(A+\eta)^2}\right)-\frac{A}{(A+\eta)}f'^2+\frac{A}{(A+\eta)}ff''+\frac{A}{(A+\eta)^2}ff'-M\varphi_1\frac{\sigma_{nf}}{\sigma_f}f'+A_1\lambda_1\varphi_1\theta, \tag{16}$$

$$\frac{1}{\Pr}\left(\frac{k_{nf}}{k_f}+Rd\right)\{(A+\eta)\theta''+\theta'\}+\frac{Rd}{\Pr}\Big[(\theta_w-1)^3(3\theta^2\theta'^2+\theta^3\theta'')+3(\theta_w-1)^2(2\theta\theta'^2+\theta^2\theta'')+3(\theta_w-1)(\theta'^2+\theta\theta'')\Big]+EcM\frac{\sigma_{nf}}{\sigma_f}f'^2+A\gamma f\theta'=0, \tag{17}$$

with boundary conditions

$$f(0)=0,\ f'(0)=1,\ \theta(0)=1\qquad f'(\infty)=0,\ f''(\infty)=0,\ \theta(\infty)=0, \tag{18}$$

where $A=R\sqrt{\frac{c}{\nu_f}}$ is the curvature parameter, $M=\frac{\sigma_f B_0^2}{\mu_f}$ is the Hartman number, $\lambda_1=\frac{Gr}{Re_s^2}$ is the mixed convection parameter, $Gr=\frac{g\beta_f(T_w-T_\infty)s^3}{\nu_f^2}$ is the Grashof number, $Re_s=\frac{as^2}{\nu_f}$ is the Reynolds number, $Ec=\frac{a^2s^2}{C_p(T_w-T_\infty)}$ is the Eckert number, $\Pr=\frac{\nu_f(\rho C_p)_f}{k_f}$ is the Prandtl number and $\theta_w=\frac{T_w}{T_\infty}$ is temperature ratio parameter. When $\theta_w=1$ we will get linear thermal radiation. Also

$$\varphi_1=\frac{1}{1-\varphi+\varphi\left(\frac{\rho_s}{\rho_f}\right)},\quad \beta_1=\frac{1}{(1-\varphi)^{5/2}\left[1-\varphi+\varphi\left(\frac{\rho_s}{\rho_f}\right)\right]},\quad \gamma=1-\varphi+\varphi\frac{(\rho C_p)_s}{(\rho C_p)_f},\quad A_1=1-\varphi+\varphi\frac{(\beta\rho)_s}{(\beta\rho)_f}. \tag{19}$$

Eliminating pressure from Eqs. (15) and (16), we have

$$(A+\eta)^3f''''+2(A+\eta)^2f'''+f'-(A+\eta)f''+\beta_1A\Big\{(A+\eta)^2ff'''-(A+\eta)^2f'f''-(A+\eta)f'^2+(A+\eta)ff''-ff'\Big\}-(1-\varphi)^{5/2}M\frac{\sigma_{nf}}{\sigma_f}\Big\{(A+\eta)^3f''+(A+\eta)^2f'\Big\}+(1-\varphi)^{5/2}A_1\lambda_1\Big\{(A+\eta)^3\theta'+(A+\eta)^2\theta\Big\}=0, \tag{20}$$

Skin friction coefficient and the local Nusselt number are

$$C_f=\frac{\tau_{rs}}{\rho_f u_w^2},\quad Nu_s=\frac{sq_w}{k_f(T_w-T_\infty)}, \tag{21}$$

in which τ_{rs} and q_w denotes surface shear stress and heat flux which are defined as:

$$\tau_{rs}=\mu_{nf}\left(\frac{\partial u}{\partial r}-\frac{u}{(r+R)}\right)_{r=0},\qquad q_w=-k_{nf}\frac{\partial T}{\partial r}\Big|_{r=0}+q_r=-(T_w-T_\infty)\sqrt{\frac{a}{\nu_f}}(1+Rd\theta_w^3)\theta'(0). \tag{22}$$

In dimensionless form skin friction coefficient and Nusselt number are

$$Re_s^{1/2}C_f=\frac{1}{(1-\varphi)^{5/2}}\left(f''(0)-\frac{f'(0)}{k}\right),\qquad Re_s^{1/2}Nu_s=-\frac{k_{nf}}{k_f}(1+Rd\theta_w^3)\theta'(0), \tag{23}$$

where Re_s is the local Reynolds number.

Solution methodology

For HAM solutions we select initial guesses and linear operators as follows

$$f_0(\eta)=e^{-\eta}-e^{-2\eta},\ \theta_0(\eta)=e^{-\eta}, \tag{24}$$

$$\mathcal{L}_f=f''''-5f''+4,\ \mathcal{L}_\theta=\theta''-\theta, \tag{25}$$

with

$$\mathcal{L}_f(c_1e^{\eta}+c_2e^{-\eta}+c_3e^{2\eta}+c_4e^{-2\eta})=0,\ \mathcal{L}_\theta(c_5e^{\eta}+c_6e^{-\eta})=0, \tag{26}$$

where c_i $(i=1-6)$ are constants. Zeroth order deformation equations are

$$(1-H)\mathcal{L}_f\left[\hat{f}(\eta;H)-f_0(\eta)\right]=H\hbar_f\mathcal{N}_f[\hat{f}(\eta;H),\hat{\theta}(\eta;H)], \tag{27}$$

$$(1-H)\mathcal{L}_\theta\left[\hat{\theta}(\eta;H)-\theta_0(\eta)\right]=H\hbar_\theta\mathcal{N}_\theta[\hat{\theta}(\eta;H),\hat{f}(\eta;H)], \tag{28}$$

where $H\epsilon$ [0,1] is the embedding parameter. Nonlinear operators are

$$\begin{aligned}\mathcal{N}_f\left[\hat{f}(\eta;H),\hat{\theta}(\eta;H)\right]=&(A+\eta)^3\tfrac{\partial^4\hat{f}(\eta;H)}{\partial\eta^4}+2(A+\eta)^2\tfrac{\partial^3\hat{f}(\eta;H)}{\partial\eta^3}+\tfrac{\partial\hat{f}(\eta;H)}{\partial\eta}\\&-(A+\eta)\tfrac{\partial^2\hat{f}(\eta;H)}{\partial\eta^2}+\beta_1A\Big((A+\eta)^2\hat{f}(\eta;H)\tfrac{\partial^3\hat{f}(\eta;H)}{\partial\eta^3}\\&-(A+\eta)^2\tfrac{\partial\hat{f}(\eta;H)}{\partial\eta}\tfrac{\partial^2\hat{f}(\eta;H)}{\partial\eta^2}-(A+\eta)\left(\tfrac{\partial\hat{f}(\eta;H)}{\partial\eta}\right)^2\\&+(A+\eta)\hat{f}(\eta;H)\tfrac{\partial^2\hat{f}(\eta;H)}{\partial\eta^2}-\hat{f}(\eta;H)\tfrac{\partial\hat{f}(\eta;H)}{\partial\eta}\Big)\\&-(1-\varphi)^{5/2}M\tfrac{\sigma_{nf}}{\sigma_f}\left((A+\eta)^3\tfrac{\partial^2\hat{f}(\eta;H)}{\partial\eta^2}+(A+\eta)^2\tfrac{\partial\hat{f}(\eta;H)}{\partial\eta}\right)\\&+(1-\varphi)^{5/2}A_1\lambda_1\left((A+\eta)^3\tfrac{\partial\hat{\theta}(\eta;H)}{\partial\eta}+(A+\eta)^2\hat{\theta}(\eta;H)\right),\end{aligned} \tag{29}$$

$$\begin{aligned}\mathcal{N}_\theta\left[\hat{\theta}(\eta,H),\hat{f}(\eta,H)\right]=&\tfrac{1}{\Pr}\left(\tfrac{k_{nf}}{k_f}+Rd\right)\left((A+\eta)\tfrac{\partial^2\hat{\theta}(\eta;H)}{\partial\eta^2}+\tfrac{\partial\hat{\theta}(\eta;H)}{\partial\eta}\right)+\tfrac{Rd}{\Pr}\Big((\theta_w-1)^3\\&\left(3\left(\hat{\theta}(\eta;H)\right)^2\left(\tfrac{\partial\hat{\theta}(\eta;H)}{\partial\eta}\right)^2+\left(\hat{\theta}(\eta;H)\right)^3\tfrac{\partial^2\hat{\theta}(\eta;H)}{\partial\eta^2}\right)+3(\theta_w-1)^2\\&\left(2\hat{\theta}(\eta;H)\left(\tfrac{\partial\hat{\theta}(\eta;H)}{\partial\eta}\right)^2+\left(\hat{\theta}(\eta;H)\right)^2\tfrac{\partial^2\hat{\theta}(\eta;H)}{\partial\eta^2}\right)+3(\theta_w-1)\\&\left(\left(\tfrac{\partial\hat{\theta}(\eta;H)}{\partial\eta}\right)^2+\left(\hat{\theta}(\eta;H)\right)\tfrac{\partial^2\hat{\theta}(\eta;H)}{\partial\eta^2}\right)\Big)+MEc\tfrac{\sigma_{nf}}{\sigma_f}\left(\tfrac{\partial\hat{f}(\eta;H)}{\partial\eta}\right)^2\\&+A\gamma\hat{f}(\eta;H)\tfrac{\partial\hat{\theta}(\eta;H)}{\partial\eta},\end{aligned} \tag{30}$$

$$\hat{f}'(0;H)=1,\ \hat{f}(0;H)=0,\ \hat{f}'(\infty;H)=0,\ \hat{f}''(\infty;H)=0 \tag{31}$$

$$\hat{\theta}(0;H)=1,\ \hat{\theta}(\infty;H)=0, \tag{32}$$

The m[th]-order deformation equations are

$$\mathcal{L}_f\left[f_m(\eta)-\chi_mf_{m-1}(\eta)\right]=\hbar_f\mathcal{R}_{f,m}(\eta), \tag{33}$$

$$\mathcal{L}_\theta\left[\theta_m(\eta)-\chi_m\theta_{m-1}(\eta)\right]=\hbar_\theta\mathcal{R}_{\theta,m}(\eta), \tag{34}$$

where

$$\chi_m=\begin{cases}0, & m\leqslant 1\\ 1, & m>1\end{cases}, \tag{35}$$

$$\begin{aligned}\mathcal{R}_{f,m}(\eta)=&(A+\eta)^3f'''_{m-1}+2(A+\eta)^2f'''_{m-1}+f'_{m-1}-(A+\eta)f''_{m-1}\\&+\beta_1A\sum_{k=0}^{m-1}\Big[(A+\eta)^2f_{m-1-k}f'''_k-(A+\eta)^2f'_{m-1-k}f''_k\\&-(A+\eta)f'_{m-1-k}f'_k+(A+\eta)f_{m-1-k}f''_k-f_{m-1-k}f'_k\Big]\\&-(1-\varphi)^{5/2}M\tfrac{\sigma_{nf}}{\sigma_f}\left((A+\eta)^3f''_{m-1}+(A+\eta)^2f'_{m-1}\right)\\&+(1-\varphi)^{5/2}A_1\lambda_1\left((A+\eta)^3\theta'_{m-1}+(A+\eta)^2\theta_{m-1}\right).\end{aligned} \tag{36}$$

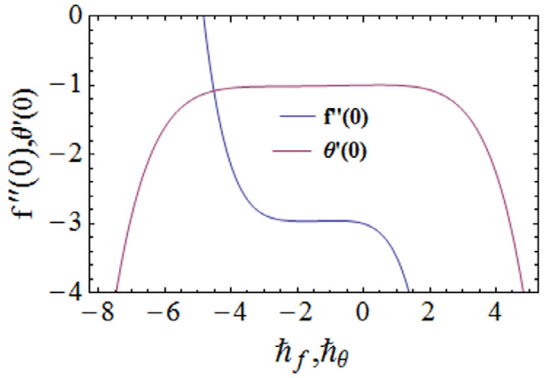

Fig. 1. $\hbar$-Curves for Cu nanoparticles when $\varphi = 0.03$, $A = M = 0.4$, $Rd = 0.3$, $\lambda_1 = 0.9$, $\theta_w = 1.1$ and $Ec = 0.6$.

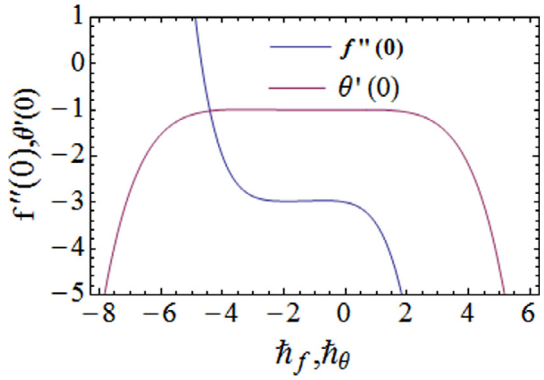

Fig. 2. $\hbar$-curves for Ag nanoparticles when $\varphi = 0.03, A = 0.4$, $M = 0.5, Rd = 0.7$, $\lambda_1 = 1.0, \theta_w = 1.1$ and $Ec = 0.4$.

Table 1
Convergence of obtained HAM solutions for Cu-water nanofluid for different order of approximations when $\varphi = 0.03, A = M = 0.4, Rd = 0.3, \lambda_1 = 0.9, \theta_w = 1.1$ and $Ec = 0.6$.

Order of approximations	$-f''(0)$	$-\theta'(0)$
1	2.980	1.000
2	2.968	1.000
4	2.959	1.000
5	2.957	1.001
6	2.956	1.001
10	2.956	1.001
30	2.956	1.001
40	2.956	1.001
45	2.956	1.001

Table 2
Convergence of obtained HAM solutions for Ag-water nanofluid for different order of approximations when $\varphi = 0.03, A = 0.4, M = 0.5, Rd = 0.7, \lambda_1 = 1.0, \theta_w = 1.1$ and $Ec = 0.4$.

Order of approximations	$-f''(0)$	$-\theta'(0)$
1	2.981	1.000
4	2.958	1.001
6	2.955	1.001
7	2.955	1.002
8	2.954	1.002
10	2.954	1.002
30	2.954	1.002
40	2.954	1.002
45	2.954	1.002

$$\begin{aligned}\mathcal{R}_{\theta,m}(\eta) &= \tfrac{1}{\Pr}\left(\tfrac{k_{nf}}{k_f} + Rd\right)\left((A+\eta)\theta''_{m-1} + \theta'_{m-1}\right)\\ &+3(\theta_w-1)\tfrac{Rd}{\Pr}\sum_{k=0}^{m-1}\left[\theta'_{m-1-k}\theta'_k + \theta_{m-1-k}\theta''_k\right]\\ &+EcM\tfrac{\sigma_{nf}}{\sigma_f}\sum_{k=0}^{m-1}f'_{m-1-k}f'_k + A\gamma\sum_{k=0}^{m-1}f_{m-1-k}\theta'_k\\ &+3(\theta_w-1)^2\tfrac{Rd}{\Pr}\sum_{l=0}^{m-1}\theta_{m-1-l}\left(2\sum_{j=0}^{l}\theta'_{l-j}\theta'_j + \sum_{j=0}^{l}\theta_{l-j}\theta''_j\right)\\ &+\tfrac{Rd}{\Pr}(\theta_w-1)^3\sum_{k=0}^{m-1}\theta_{m-1-k}\sum_{l=0}^{k}\theta_{k-1}\sum_{s=0}^{l}\left(3\theta'_{l-s}\theta'_s + \theta_{l-s}\theta''_s\right),\end{aligned} \tag{37}$$

$$f'_m(0) = f_m(0) = f'_m(\infty) = f''_m(\infty) = \theta_m(0) = \theta_m(\infty) = 0. \tag{38}$$

The general solutions (f_m, θ_m) comprising the special solutions (f^*_m, θ^*_m) are

$$\begin{aligned}f_m(\eta) &= f^*_m(\eta) + c_1e^{\eta} + c_2e^{-\eta} + c_3e^{2\eta} + c_4e^{-2\eta},\\ \theta_m(\eta) &= \theta^*_m(\eta) + c_5e^{\eta} + c_6e^{-\eta},\end{aligned} \tag{39}$$

where $c_1 - c_6$ are constants.

Convergence analysis

HAM is a method to solve nonlinear ordinary differential equations. It provides convenient way to select the basic functions of the desired solution and the corresponding auxiliary linear operator. The auxiliary parameters $\hbar_f$ and $\hbar_\theta$ give freedom to provide convergent series solutions. $-1.5 \leqslant \hbar_f \leqslant -0.1$ and $-0.8 \leqslant \hbar_\theta \leqslant 0.1$ are ranges of the auxiliary parameters for Cu nanoparticles. The ranges of the auxiliary parameters for Ag nanoparticles are $-1 \leqslant \hbar_f \leqslant 0.1$, and $-1.9 \leqslant \hbar_\theta \leqslant 0.1$. Also the region of convergence for HAM solutions is $0 < \eta < \infty$when $\hbar_f = -0.8$ and $\hbar_\theta = -0.2$ for Cu nanoparticles and for Ag nanoparticles when $\hbar_f = -0.9$ and $\hbar_\theta = -1$ (Figs. 1 and 2) (Tables1–3).

Results and discussion

Dimensionless velocity profiles

Fig. 3 depicts the behavior of curvature parameter A on velocity profile $f'(\eta)$. Larger values of curvature parameter enhance the velocity profile. Because radius of sheet increases for higher values of curvature parameter which enhances the motion of the fluid. Fig. 4 shows the effect of Hartman number M on $f'(\eta)$. Velocity profile $f'(\eta)$ decreases when Hartman number is increased. It is because the Lorentz force produces for larger M which enhances the resistance to the fluid flow. Fig. 5 shows the behavior of mixed convection parameter λ_1 on velocity profile $f'(\eta)$. Here velocity profile is increasing function of mixed convection parameter λ_1.

Dimensionless temperature profiles

Fig. 6 is plotted to show the behavior of curvature parameter A on temperature profile $\theta(\eta)$. Here larger values of curvature parameter reduce the temperature profile $\theta(\eta)$. Temperature profiles are plotted for different values of radiation parameter Rd (see Fig. 7). Increasing radiation parameter enhances the radiative heat flux which produces heat so increase in the temperature profile is observed. Fig. 8 exhibits the variation of temperature parameter θ_w on temperature profile $\theta(\eta)$. Larger values of temperature parameter θ_w correspond to increase in the temperature profile $\theta(\eta)$. Fig. 9 shows the impact of nanoparticles volume fraction

Table 3
Some thermophysical properties of base fluid and nanoparticles.

	$\rho(kg/m^3)$	$C_p(j/kgK)$	$k(W/mK)$	$\beta \times 10^5(K^{-1})$	$\sigma(\Omega m)^{-1}$
Water (H_2O)	997.1	4179	0.613	21	0.05
Copper (Cu)	8933	385	401	1.67	5.96×10^7
Silver (Ag)	10,500	235	429	1.89	6.3×10^7

φon temperature profile $\theta(\eta)$. There is an enhancement in temperature profile $\theta(\eta)$ when nanoparticles volume fraction $\varphi$is increased. Because the thermal conductivity increases for larger value of volume of nanoparticles. Fig. 10 depicts the behavior of Eckert number Ec on temperature profile $\theta(\eta)$. When we increase

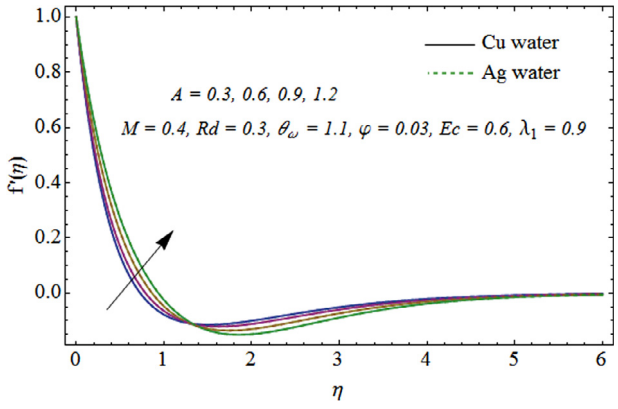

Fig. 3. Behavior of A on $f'(\eta)$.

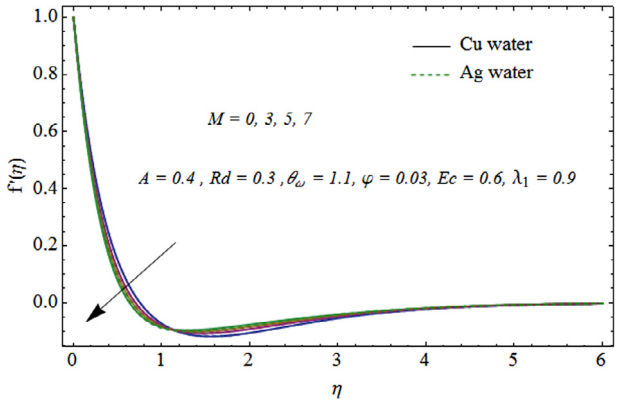

Fig. 4. Behavior of M on $f'(\eta)$.

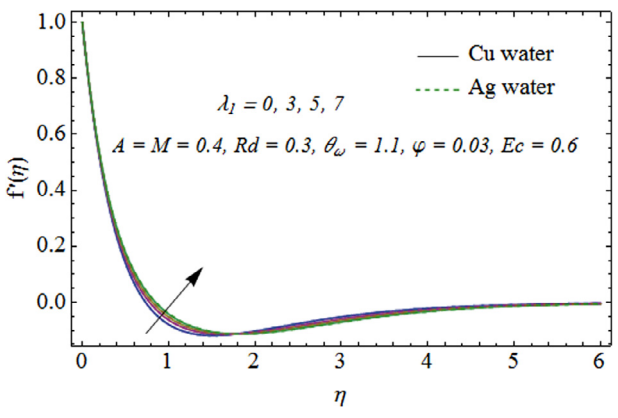

Fig. 5. Behavior of λ_1 on $f'(\eta)$.

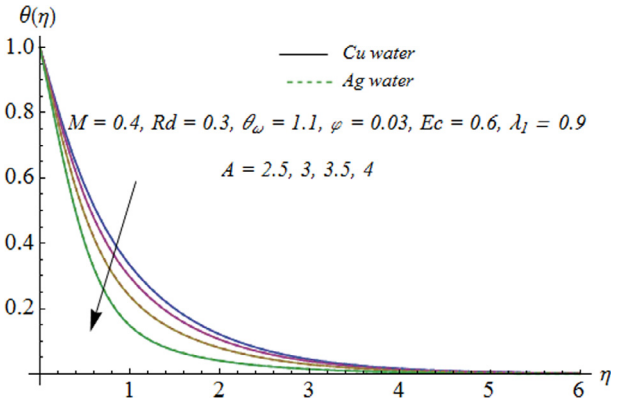

Fig. 6. Behavior of A on $\theta(\eta)$.

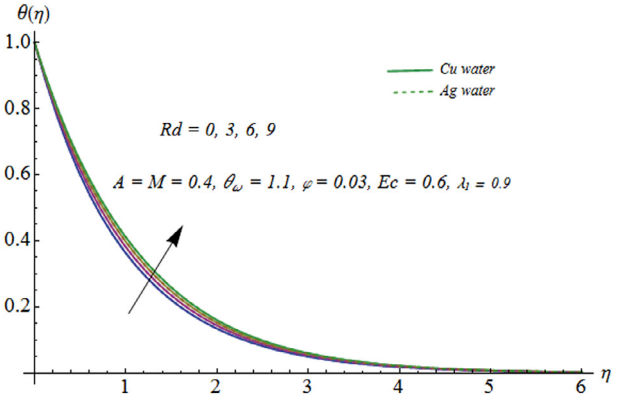

Fig. 7. Behavior of Rd on $\theta(\eta)$.

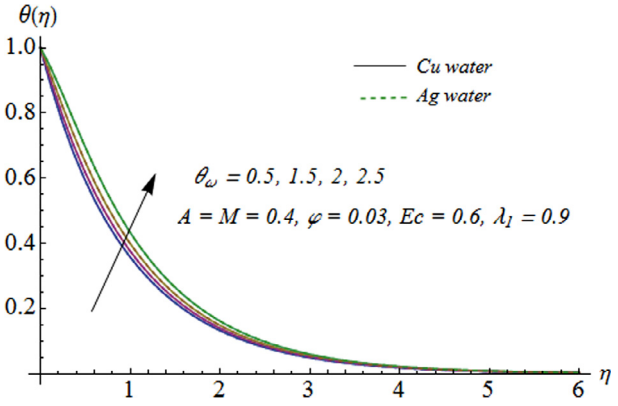

Fig. 8. Behavior of θ_w on $\theta(\eta)$.

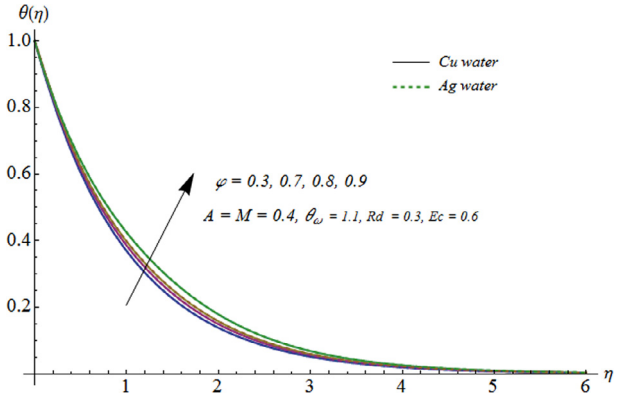

Fig. 9. Behavior of φ on $\theta(\eta)$.

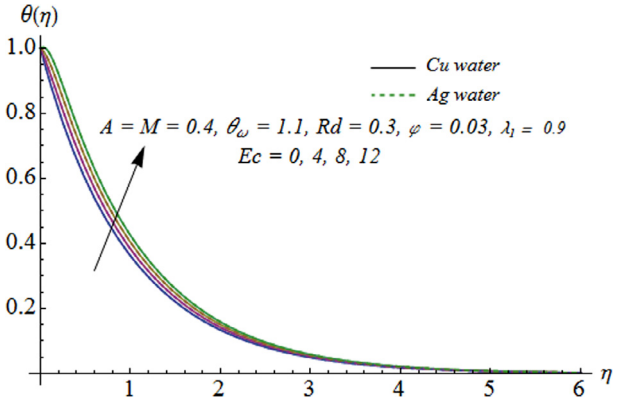

Fig. 10. Behavior of Ec on $\theta(\eta)$.

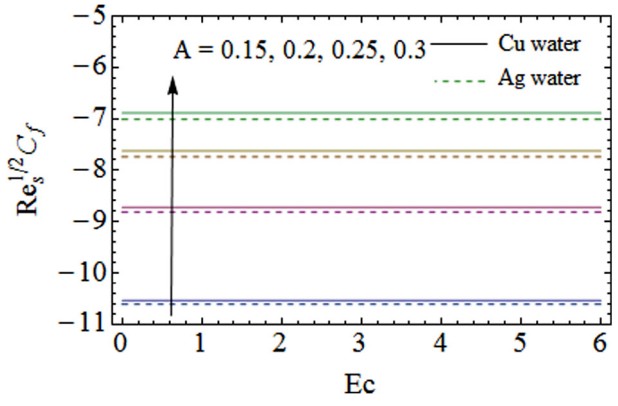

Fig. 11. Behavior of A on $Re_s^{1/2}C_f$.

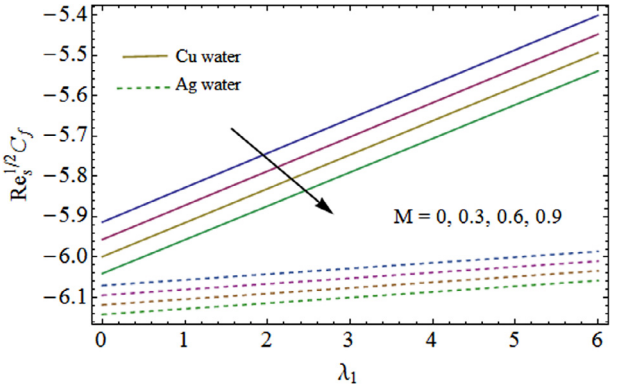

Fig. 12. Behavior of M on $Re_s^{1/2}C_f$.

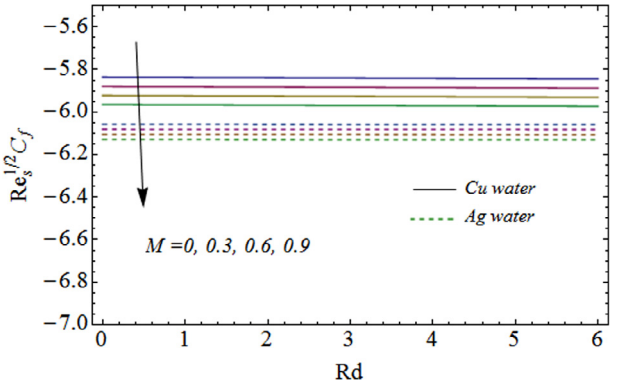

Fig. 13. Behavior of M on $Re_s^{1/2}C_f$.

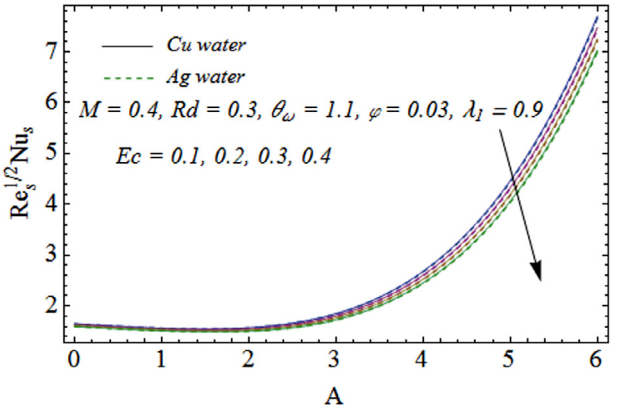

Fig. 14. Behavior of Econ $Re_s^{1/2}Nu_s$.

the Eckert number Ec the temperature profile $\theta(\eta)$ enhances. As Eckert number is the ratio of kinetic energy to enthalpy. Kinetic energy increases for higher values of Eckert number Ec hence temperature profile $\theta(\eta)$ increases.

Skin friction coefficient

Behavior of curvature parameter A on skin friction coefficient $Re_s^{1/2}C_f$ via Eckert number Ec is shown in Fig. 11. Here magnitude of surface drag force decreases for increasing values of curvature parameter A. Fig. 12 illustrates the effects of Hartman number M via mixed convection parameter λ_1 on skin friction coefficient. Increasing values of Hartman number enhance the skin friction coefficient. Fig. 13 depicts the behavior of Hartman number M against radiation parameter Rd on skin friction coefficient. Surface drag force increases for larger values of Hartman number M.

Nusselt number

Fig. 14 illustrates the behavior of Eckert number Ec on Nusselt number $Re_s^{1/2}Nu_s$ against curvature parameter A. For higher values of Eckert number surface heat transfer rate reduce. Fig. 15 illustrates the impact of radiation parameter Rd via curvature parameter A. Nusselt number enhances for larger values of radiation parameter. Effect of temperature parameter θ_w via radiation parameter is displayed in Fig. 16. Surface heat transfer rate increases for increasing values of temperature parameter.

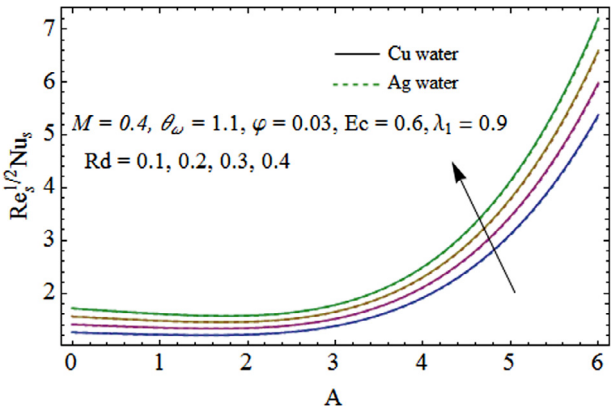

Fig. 15. Behavior of Rd on $Re_s^{1/2}Nu_s$.

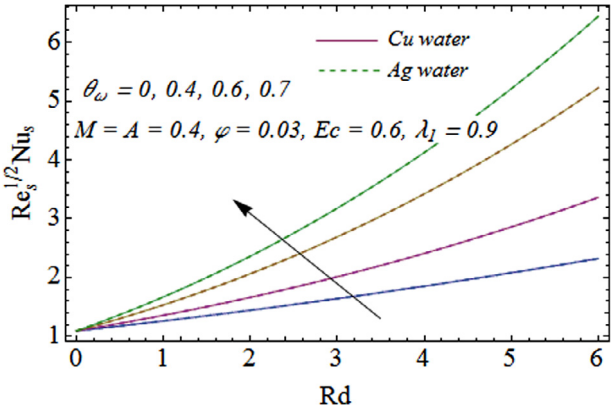

Fig. 16. Behavior of θ_w on $Re_s^{1/2}Nu_s$.

Main results

MHD flow of nanofluid with nonlinear thermal radiation and mixed convection over a curved stretching sheet is investigated here. The main points are as follows:

- Opposite impact of curvature parameter and Hartman number is seen on the velocity profile.
- Increasing values of radiation parameter enhance the temperature profile.
- Surface drag force is higher for silver-water nanofluid as compared to copper–water nanofluid.
- Surface heat transfer rate is proportional to radiation and temperature parameters.

References

[1] Choi SUS. Enhancing thermal conductivity of fluids with nanoparticles. In: Proceedings of the ASME Int. Mech. Eng. Cong. Exposi. 66; 1995:99–105.
[2] Tiwari RK, Das MK. Heat transfer augmentation in a two-sided lid-driven differentially heated square cavity utilizing nanofluids. Int J Heat Mass Transfer 2007;50:2002–18.
[3] Turkyilmazoglu M. Nanofluid flow and heat transfer due to a rotating disk. Comput Fluids 2014;94:139–46.
[4] Vajravelu K, Prasad KV, Lee J, Lee C, Pop I, Gorder RAV. Convective heat transfer in the flow of viscous Ag-water and Cu-water nanofluids over a stretching surface. Int J Therm Sci 2011;50:843–51.
[5] Hayat T, Imtiaz M, Alsaedi A. Impact of magnetohydrodynamics in bidirectional flow of nanofluid subject to second order slip velocity and homogeneous–heterogeneous reactions. J Magn Magn Mater 2015;395:294–302.
[6] Sheikholeslami M, Ganji DD, Javed MY, Ellahi R. Effect of thermal radiation on magnetohydrodynamics nanofluid flow and heat transfer by means of two phase model. J Magn Magn Mater 2015;374:36–43.
[7] Abbasi FM, Hayat T, Ahmad B. Peristaltic transport of copper–waternanofluid saturating porous medium. Physica E 2015;67:47–53.
[8] Hayat T, Imtiaz M, Alsaedi A, Alzahrani F. Effects of homogeneous–heterogeneous reactions in flow of magnetite-Fe_3O_4 nanoparticles by a rotating disk. J Mol Liq 2016;216:845–55.
[9] Mansur S, Ishak A. Unsteady boundary layer flow of a nanofluid over a stretching/shrinking sheet with a convective boundary condition. J. Egypt Math Soc 2016;24:650–5 (in press).
[10] Makinde OD, Mabood F, Khan WA, Tshehla MS. MHD flow of a variable viscosity nanofluid over a radially stretching convective surface with radiative heat. J Mol Liq 2016;219:624–30.
[11] Dogonchi AS, Ganji DD. Investigation of MHD nanofluid flow and heat transfer in a stretching/shrinking convergent/divergent channel considering thermal radiation. J Mol Liq 2016;220:592–603.
[12] Ibanez G, Lopez A, Pantoja J, Moreira J. Entropy generation analysis of a nanofluid flow in MHD porous microchannel with hydrodynamic slip and thermal radiation. Int J Heat Mass Transfer 2016;100:89–97.
[13] Sheikholeslami M, Hatami M, Domairry G. Numerical simulation of two phase unsteady nanofluid flow and heat transfer between parallel plates in presence of time dependent magnetic field. J Taiwan Inst Chem Eng 2015;46:43–50.
[14] Asghar S, Hayat T, Shafiq A, Alsaedi A. Effect of inclined magnetic field in flow of third grade fluid with variable thermal conductivity. AIP Adv 2015;5:087108.
[15] Rashidi MM, Ali M, Freidoonimehr N, Rostami B, Hossian A. Mixed convection heat transfer for viscoelastic fluid flow over a porous wedge with thermal radiation. Adv Mech Eng 2014;204:735939.
[16] Mukhopadhyay S. Slip effects on MHD boundary layer flow over an exponentially stretching sheet with suction/blowing and thermal radiation. Ain Shams Eng J 2013;4:485–91.
[17] Bhattacharyya K, Mukhopadhyay S, Layek GC, Pop I. Effects of thermal radiation on micropolar fluid flow and heat transfer over a porous shrinking sheet. Int J Heat Mass Transfer 2012;55:2945–52.
[18] Makinde OD. Second law analysis for variable viscosity hydromagnetic boundary layer flow with thermal radiation and Newtonian heating. Entropy 2011;13:1446–64.
[19] Magyari E. Comment on "Mixed convection boundary layer flow over a horizontal plate with thermal radiation". Heat Mass Transfer 2010;46:809–10. by A. Ishak, Heat and Mass Transfer, DOI http://dx.doi.org/10.1007/s00231-009-0552-3.
[20] Hayat T, Imtiaz M, Alsaedi A, Kutbi MA. MHD three-dimensional flow of nanofluid with velocity slip and nonlinear thermal radiation. J Magn Magn Mater 2015;396:31–7.
[21] Hayat T, Muhammad T, Alsaedi A, Alhuthali MS. Magnetohydrodynamic three-dimensional flow of viscoelastic nanofluid in the presence of nonlinear thermal radiation. J Magn Magn Mater 2015;385:222–9.
[22] Mustafa M, Mushtaq A, Hayat T, Alsaedi A. Model to study the non-linear radiation heat transfer in the stagnation-point flow of power-law fluid. Int J Numer Methods Heat Fluid Flow 2015;25:1107–19.
[23] Shehzad SA, Hayat T, Alsaedi A, Obid MA. Nonlinear thermal radiation in three-dimensional flow of Jeffrey nanofluid: a model for sol Computar energy. Appl Math 2014;248:273–86.
[24] Mushtaq A, Mustafa M, Hayat T, Alsaedi A. Nonlinear radiative heat transfer in the flow of nanofluid due to solar energy: a numerical study. J Taiwan Inst Chem Eng 2014;45:1176–83.
[25] Cortell R. Fluid flow and radiative nonlinear heat transfer over stretching sheet. J King Saud Univ Sci 2013;26:161–7.
[26] Pantokratoras A, Fang T. Sakiadis flow with nonlinear Rosseland thermal radiation. Phys Scr 2013;87:015703.
[27] Farooq U, Zhao YL, Hayat T, Alsaedi A, Liao SJ. Application of the HAM-based mathematica package BVPh 2.0 on MHD Falkner-Skan flow of nanofluid. Comput Fluids 2015;111:69–75.
[28] Abbasbandy S, Yurusoy M, Gulluce H. Analytical solutions of non-linear equations of power-law fluids of second grade over an infinite porous plate. Math Comput Appl 2014;19(2):124.
[29] Hatami M, Nouri R, Ganji DD. Forced convection analysis for MHD Al2O3-water nanofluid flow over a horizontal plate. J Mol Liq 2013;187:294–301.
[30] Turkyilmazoglu M. Solution of the Thomas-Fermi equation with a convergent approach. Commun Nonlinear Sci Numer Simul 2012;17:4097–103.
[31] Arqub OA, El-Ajou A. Solution of the frictional epidemic model by homotopy analysis method. J King Saud Univ Sci 2013;25:73–81.
[32] Ellahi R, Hassan M, Zeeshan A. Shape effects of nanosize particles in Cu–H_2O nanofluid on entropy generation. Int J Heat Mass Transfer 2015;81:449–56.
[33] Hayat T, Qayyum S, Imtiaz M, Alsaedi A. Impact of Cattaneo-Christov heat flux model on Jeffrey fluid flow with homogeneous-heterogeneous reaction. PLOS One 2016;11(2):e0148662.
[34] Hayat T, Rashid M, Imtiaz M, Alsaedi A. Magnetohydrodynamic (MHD) stretched flow of nanofluid with power-law velocity and chemical reaction. AIP Adv 2015;5:117121.
[35] Brinkman HC. The viscosity of concentrated suspensions and solutions. J Chem Phys 1952;20:571–81.
[36] Cebeci T, Bradshaw P. Physical and computational aspects of convective heat transfer. New York: Springer-Verlag; 1988 (Chapter 13).
[37] Maxwell JC. A treatise on electricity and magnetism. Cambridge Oxford University Press; 1904.